Eur. Phys. J. Appl. Phys. **95**, 10201 (2021)

https://doi.org/10.1051/epjap/2021210090

THE EUROPEAN PHYSICAL JOURNAL APPLIED PHYSICS

Regular Article

New tailored organic semiconductors thin films for optoelectronic applications★

Dinesh Pathak[1,*], Sanjay Kumar[2], Sonali Andotra[1], Jibin Thomas[1], Navneet Kaur[3], Praveen Kumar[4], and Vaneet Kumar[5]

[1] Department of Physics, Sri Sai University, Palampur, Himachal Pradesh, India
[2] Institute of Physics, Faculty of Science, University of South Bohemia, Ceske Budejovice, Czech Republic
[3] Department of Chemistry, Panjab University, Chandigarh, India
[4] Department of Physics, D.A.V University, Jalandhar, Punjab, India
[5] Department of Applied Sciences, CT Group of Institutions, Jalandhar, Punjab, India

Received: 16 April 2021 / Received in final form: 30 May 2021 / Accepted: 8 June 2021

Abstract. In this study, we have investigated new tailored organic semiconductor materials for optoelectronic application, such as organic solar cells. The carbon-based organic semiconductor material has promising advantages in organic thin-film form. Moreover, due to its low cost, organic thin films are suitable and cheaper than inorganic thin-film. The bandgap of organic semiconductors materials can be tuned and mostly lies between 2.0 eV and 4 eV and the optical absorption edge of organic semiconductors typically lies in between 1.7 eV and 3 eV. They can be easily tailored by modifying the carbon chain and legends and looks promising for engineering the bandgap to harness the solar spectrum. In this work, with new tailored organic semiconductors, the solution route is explored which is a low-cost processing method. (Anthracen-9-yl) methylene naphthalene-1-amine; 4-(anthracen-9-ylmethyleneamino)-1,5dimethyl-2-phenyl-1H-pyrazol-3-one and N-(anthracen-9-ylmethyl)-3, 4-dimethoxyaniline thin-films are processed by spin coating method with changing concentration such as 0.05 wt.% and 0.08 wt.%. Thin films of organic semiconductors were prepared on the glass substrate and annealed at 55 °C. The structural and optical behavior of (Anthracen-9-yl) methylene naphthalene-1-amine, 4-(anthracen-9-ylmethyleneamino)-1,5dimethyl-2-phenyl-1H-pyrazol-3-one, and N-(anthracen-9-ylmethyl)-3, 4-dimethoxyaniline organic semiconductors thin films is studied by X-ray diffraction (XRD), Scanning electron microscopy (SEM) and UV-Visible spectroscopy technique. The XRD data of the synthesized sample suggests the nano crystallinity of the organic layers. And, the SEM micrographs show the dense packing when we increase the wt.% 0.05 to 0.08. Additionally, analysis of the optical absorption measurements found that the engineered bandgap of synthesized thin films are 2.18 eV, 2.35 eV, 2.36eV, 2.52eV, and 2.65eV which suggest suitability for applications of optoelectronic devices such as solar cell. Such lightweight, eco-friendly and disposable new carbon-based materials seem to have the potential to replace other traditional hazardous heavy materials for future eco-friendly flat fast electronics.

1 Introduction

The increase in energy demand and limited availability of fossils has forced the scientific community to move toward renewables. Sun is most promising in this discussion and harnessing energy from the sun requires materials. Organic materials appear to be better as compared to inorganic materials due to advantages such as easy production, tailoring possibilities, lightweight, and friendly behavior toward the environment [1–3]. Recent advances in organic thin-film semiconductor devices have gained a lot of attention as flexible and economical in comparison to silicon-based devices [4–9]. Organic semiconductors are polymers molecules that are composed of carbon and hydrogen atoms. Due to the many benefits of organic semiconductors such as mechanical strength, flexibility, and easy fabrication, the possibility of tailoring in a wide range, they are used in many electronic devices, e.g. organic solar cells [10–13], electroluminescent devices [14,15], organic field-effect transistor [16–22] and organic light-emitting diodes [23–25], etc. In addition, organic semiconductors are being engineered more conducting by doping with strong electrons donor or acceptor [26,27], for example, doped light-emitting diode [28–30] and doped polyacetylene [31,32]. Natural organic semiconductors in the form of polyfluorene-primarily based have been substantially studied and used in light-emitting diodes [33–35]. In spite of achieving high efficiency in OPVs, yet there is a wide need for improvements e.g. the need of

★ Contribution to the Topical Issue "Advanced Materials for Energy Harvesting, Storage, Sensing and Environmental Engineering (ICOME 2019)", edited by Mohammed El Ganaoui, Mohamed El Jouad, Rachid Bennacer, Jean-Michel Nunzi.

* e-mail: dineshpathak80@gmail.com

electron-acceptor materials other than fullerene, new tailored molecules, a better understanding of the charge-transport mechanism in organic materials, a requirement of the material compatible with the flexible substrate, durability of the organic materials-based devices, etc. [36]. Bulk heterojunction photovoltaic cell is another class of devices, known as fourth-generation electronics devices which are believed to be dominating in the energy sector in future [37–39]. Many fabrication methods have been used for the deposition of thin films as well as organic semiconductor thin films, such as dip coating [40–42], thermal evaporation, sputtering and CVD [43–51].

Keeping the above issues in mind new tailored organic semiconductors were processed by a low-cost technique that has potential for industrial scale-up. Processing, structural and optical properties of these new semiconductors are presented in this communication for applications in future eco-friendly fast flat optoelectronic devices. Moreover, the novelty of this research is to deposit the newly tailored organic semiconductor material (a) Anthracen-9-yl)methylene naphthalene-1-amine, (b) 4-(anthracen-9-ylmethylene amino)-1,5-dimethyl-2-phenyl-1H-pyrazol-3-one, and (c) N-(anthracen-9-ylmethyl)-3,4-dimethoxyaniline in the form of thin films by a low-cost spin coating method and to investigate the influence of different concentrations of solute in wt.% 0.05 and 0.08 on the systems and on the structural, morphological and optical properties of the thin films. We hope that these data certainly be helpful as a scientific or technical basis in organic semiconductor processing and photovoltaic technology.

2 Experimental

2.1 Material used

(a) (Anthracen-9-yl)methylene naphthalene-1-amine (9)

Schiff base 9 was synthesized following a previously reported procedure [52]. The anthracene-9-carboxaldehyde (0.50 g, 2.42 mmol) solution in absolute C_2H_5OH was refluxed for 10 min. To the refluxing solution, the solution of 2-naphthylamine (0.345 g, 2.42 mmol) in absolute C_2H_5OH, was added. For 3 hours, the reaction mixture was refluxed. After the reaction was completed (TLC), the mixture was cooled down and then filtered off to get the crude product. The crude solid was recrystallized from $CHCl_3$ solution to get pure yellow-colored organic semiconductor compound 9.

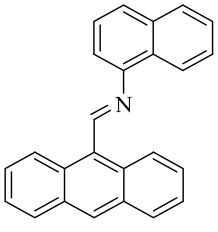

9

Yellow solid, yield (%) 70; m.p.: 160–162 °C; **FT-IR** (cm^{-1}) 1601 ($\nu_{C=N}$); **^{1}H NMR** ($CDCl_3$, 400 MHz) δ (ppm): 9.78 (s, 1H, Ar-H), 8.91 (d, 2H, Ar-H, $J = 8.8$ Hz), 8.56 (s, 1H, N=CH), 8.43 (d, 1H, Ar-H, $J = 7.76$ Hz), 8.04 (d, 2H, Ar-H, $J = 8.28$ Hz), 7.84 (dd, 2H, Ar-H, $J_1 = 7.52$ Hz, $J_2 = 8.24$ Hz), 7.59–7.49 (m, 7H, Ar-H), 7.25 (d, 1H, Ar-H, $J = 7.16$ Hz).

(b) 4-(Anthracen-9-ylmethylene amino)-1,5-dimethyl-2-phenyl-1H-pyrazol-3-one (10)

To stirring a solution of anthracene-9-carboxaldehyde (0.50 g, 2.42 mmol) and ethanolic solution of 4-amino-antipyrine (0.92 g, 2.42 mmol) was added and then allowed to reflux. The progress of the reaction was monitored through (TLC) and was completed in approximately 3 hours. The reaction of the mixture was filtered through the crucible and then washed two times with CH_3OH to get orange-colored compound 10.

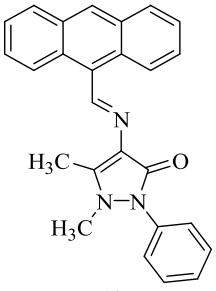

10

Orange solid, yield (%) 82; m.p.: 171–173 °C; **FT-IR** (cm^{-1}) 1637 ($\nu_{C=N}$); **^{1}H NMR** ($CDCl_3$, 400 MHz) δ (ppm): 11.07 (s, 1H, Ar-H), 8.98 (d, 2H, Ar-H, $J = 8.64$ Hz), 8.49 (s, 1H, N=CH), 8.03 (d, 2H, Ar-H, $J = 8$ Hz), 7.57–7.48 (m, 8H, Ar-H), 7.38 (t, 1H, Ar-H, $J = 7.52$ Hz, $J = 7.85$ Hz), 3.21 (s, 3H, $-CH_3$), 2.57 (s, 3H, $-CH_3$); **^{13}C NMR** ($CDCl_3$, 100 MHz) δ (ppm):150.15, 143.47, 141.90, 131.53, 130.45, 129.49, 129.14, 127.92, 126.47, 125.17, 124.19, 113.29, 103.08, 98.87, 55.82, 55.77, 41.67; **ESI-MS**: m/z (assignment) = 392.38 [$(M+1)^+$].

(c) N-(Anthracen-9-ylmethyl)-3,4-dimethoxyaniline (8)

Reduced Schiff base **8** was synthesized following a previously reported procedure [53]. To stir solution of Schiff base N-(Anthracen-9-ylmethylene)-3,4-dimethoxyaniline (0.5 g, 1.45 mmol) in absolute C_2H_5OH at room temperature, $NaBH_4$ (0.082 g, 2.175 mmol) was added and then the color of solution was observed when immediate it was changed from orange to yellow. The progress of the reaction was monitored through TLC and it was observed that the reaction gets fully completed in 1 hour. The reaction mixture was poured in ice-cold water in order to remove excess of $NaBH_4$ and then filtered off to obtain a crude product. The crude solid was recrystallized from $CHCl_3$ to get **8** in its pure form.

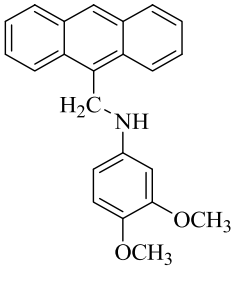

8

Table 1. Amount of solute with wt% 0.05 for material 'a', 'b', 'c' in sample set-I, and wt% 0.08 for material 'a', 'b' in sample set-II.

Sr. no.	Material	Sample name	Amount of solute (wt% 0.05) (Sample set-I)	Amount of solute (wt% 0.08) (Sample set-II)
(1)	(Anthracen-9-yl)methylene naphthalene-1-amine	Material-a	0.09942 g	0.0795 g
(2)	4-(anthracen-9-ylmethylene amino)-1, 5-dimethyl-2-phenyl-1H-pyrazol-3-one	Material-b	0.11744 g	0.0939 g
(3)	N-(anthracen-9-ylmethyl)-3,4-dimethoxyaniline	Material-c	0.10302 g	–

Yellow solid, yield (%) 84; m.p.: 172–174 °C; **FT-IR** (cm^{-1}) 3399 ($\nu_{N\text{-}H}$) 1136 ($\nu_{C\text{-}O}$); **^{1}H NMR** ($CDCl_3$, 400 MHz) δ (ppm): 8.49 (s, 1H, Ar-H), 8.31 (d, 2H, Ar-H, $J = 8.56$ Hz), 8.06 (d, 2H, Ar-H, $J = 7.76$ Hz), 7.53 (p, 4H, Ar-H, $J_1 = 6.48$ Hz, $J_2 = 7.44$), 6.89 (d, 1H, Ar-H, $J = 8.44$), 6.43 (dd, 1H, Ar-H, $J_1 = 2.48$ Hz, $J_2 = 8.48$), 6.38 (d, 1H, Ar-H, $J = 2.44$ Hz), 5.14 (s, 2H, $-CH_2$), 3.90 (s, 3H, $-OCH_3$), 3.06 (s, 3H, $-OCH_3$); **^{13}C NMR** ($CDCl_3$, 100 MHz) δ (ppm): 150.17, 143.50, 141.91, 131.53, 130.45, 129.50, 129.13, 127.91, 126.47, 125.42, 125.16, 124.18, 113.35, 103.10, 98.88, 56.83, 55.77, 41.68; **ESI-MS**: m/z [assignment]=342.36 [$(M+1)^+$].

2.2 Technique used

The low-cost easy spin coating technique is used for the deposition of organic thin films because this method produces high-quality thin films as compared to the dip-coating method. In this experiment, standard glass substrates were used. The substrates and associated beakers were washed with a soap solution, distilled water, and ultrasonically cleaned in methanol, acetone, and then isopropyl alcohol. Then, it was dried in air for 10 minutes and heated in an oven at 100 °C for 5 minutes. After conducting various trials, we found that chloroform is a suitable solvent for material-a: ($C_{25}H_{17}N$), material-b: ($C_{26}H_{21}N_3O$), and material-c: ($C_{23}H_{21}NO_2$). The solutions were prepared in two weight percentages, i.e. 0.05 and 0.08. For the first set of samples, all these 3 materials were used to prepare the solution with a weight percentage of 0.05 and the total amount of solution was fixed as 6 ml. The amount of solute was calculated by acid and base molarity calculator. For the second set of samples, only material-a and material-b were used to prepare the solution with a weight percentage of 0.08, and the total amount of the solution was fixed as 3 ml. The amount of solute for wt.% 0.05 and 0.08 is calculated as shown in Table 1. For sample c ($C_{23}H_{21}NO_2$) at higher concentation wt.% no significant changes are observed and was not studied therefore.

Moreover, preliminary arrangements on the spin coating machine were done before the final deposition. The power connection is checked and the vacuum pump was connected with the spin coater. The spinning area is cleaned and the surroundings were protected by covering the area with foil paper. The optimized rotation speed was fixed at 1000 rpm and the glass substrate was fixed on top of the spin coater. For the first set of samples, three different solutions were prepared with a weight percentage of 0.05 and the total amount of solution 6 ml is used. Two or three drops of the prepared solution were dropped over that. Then, the spin coating machine was started and after some time the first layer is formed, and then prepared thin films were annealed at 50–60 °C for crystallization. The process was repeated again and again and then 14 layers were applied to the glass substrate. The thin films of all the organic material were prepared in the same manner, having the same rotation speed 1000 rpm, and then annealed at 55 °C for 1 hour. For the second set of samples, the weight percentage was 0.08 and the total amount of solution was 3 ml was used, and the rotation speed was fixed as well as 1000 rpm. Finally, 12 layers were formed and annealed at 55 °C for one hour for crystallization. The as-prepared thin films are shown in Figure 1.

For structural and morphological investigation the films were subjected to an X-ray diffractometer machine as installed at the Indian Institute of Technology, Mandi Model number Shimazdu Lab XRD-6100, Scanning electron microscopy FEI Quanta 450 FEG, optical investigations were carried out in range 200–1100 nm to analyze absorption edges and bandgap.

3 Result and discussion

3.1 XRD characterization

XRD has good potential for the analysis of phase identification, the extent of orderness, etc. for structures because the width, sharpness, and shape of reflections yield information about the structure of the materials [54]. Figure 2 depicts the XRD spectra for tailored organic semiconductors thin film of three different deposited flat materials. It shows the XRD graph of material-a, material-b, material-c with wt.% 0.05, and material-a, material-b with wt.% 0.08. The intensity in arbitrary units versus $2\boldsymbol{\Theta}$ curves was plotted. From the graph patterns, we observed that the materials were Nano textured because all the graphs have broad peaks.

The average particle size has been found using Debye-Scherer formula:

$$D = 0.9\lambda/\beta \operatorname{Cos}\theta$$

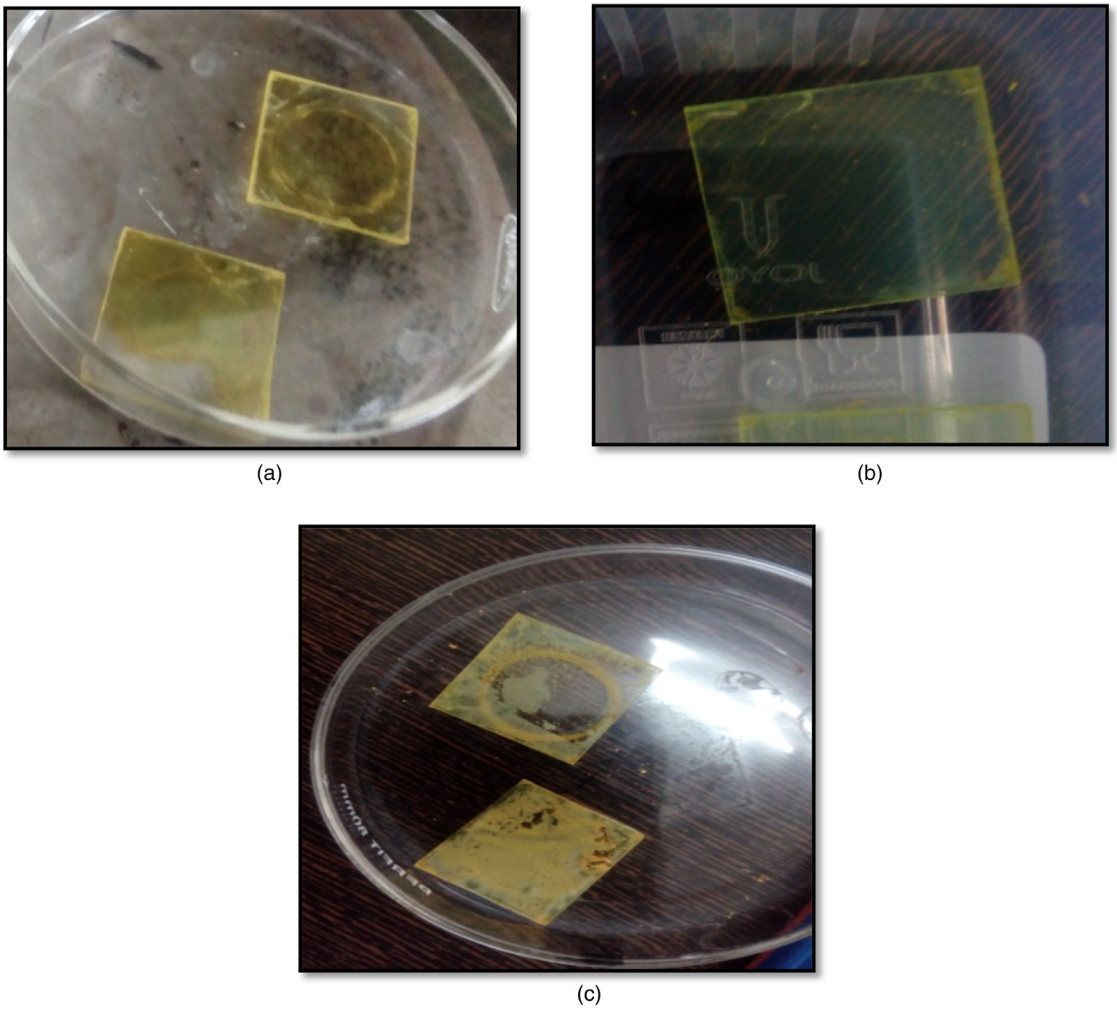

Fig. 1. Prepared thin films of new tailored organic semiconductors.

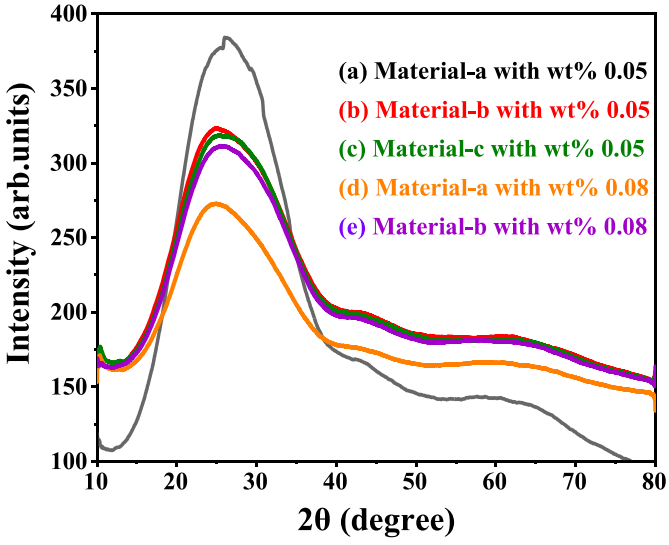

Fig. 2. XRD graph of **(a)** material-a: Anthracen-9-yl)methylene naphthalene-1-amine with wt% 0.05, **(b)** material-b: 4-(anthracen-9-ylmethylene amino)-1,5-dimethyl-2-phenyl-1H-pyrazol-3-one with wt% 0.05, **(c)** material-c: N-(anthracen-9-ylmethyl)-3,4-dimethoxyaniline with wt% 0.05 and **(d)** material-a: Anthracen-9-yl)methylene naphthalene-1-amine with wt% 0.08, **(e)** material-b: 4-(anthracen-9-ylmethylene amino)-1,5-dimethyl-2-phenyl-1H-pyrazol-3-one with wt% 0.08.

Table 2. Particle size of (a) Anthracen-9-yl)methylene naphthalene-1-amine, **(b)** 4-(anthracen-9-ylmethyleneamino)-1, 5-dimethyl-2-phenyl-1H-pyrazol-3-one, and **(c)** N-(anthracen-9-ylmethyl)-3,4-dimethoxyaniline.

Sr. no.	Materials	Sample	Particle size (nm)
(1)	(Anthracen-9-yl)methylene naphthalene-1-amine	Material-a with wt % 0.05	7.417474901
(2)	4-(anthracen-9-ylmethylene amino)-1,5-dimethyl-2-phenyl-1H-pyrazol-3-one	Material-b with wt % 0.05	11.87599461
(3)	N-(anthracen-9-ylmethyl)-3,4-dimethoxyaniline	Material-c with wt % 0.05	11.59106538
(4)	(Anthracen-9-yl)methylene naphthalene-1-amine	Material-a with wt % 0.08	10.14586658
(5)	4-(anthracen-9-ylmethylene amino)-1,5-dimethyl-2-phenyl-1H-pyrazol-3-one	Material-b with wt % 0.08	11.38316432

where 'λ' is the wavelength of X-rays, 'β' is the full width at half maxima (FWHM) in radians and '$\boldsymbol{\Theta}$' is Bragg's angle. Thus, we investigated that, the particle size of three different materials along with wt.% 0.05 and 0.08 has increased. Grain/ particle growth depends on many factors such as temperature, pressure and thermodynamics of compounds. Small decrease in particle size for material-b unlike a may be because of its chemical structure and defects due to it. These results conclude that the change in concentration and different structures of organic material plays a crucial role to get nanomaterials that are possibly better for the improvement of optoelectronic applications like solar cells. The average particle sizes are calculated from the graph and it is shown in Table 2. The combined XRD graph is shown in Figure 2.

3.2 Morphological investigation by scanning electron microscopy

Scanning electron microscopy is a unique and versatile characterization technique to analyze the surface morphology of thin-film and to determine the grain size of the materials. Figure 3 shows that SEM images of annealed organic thin films on glass substrate at wt.% 0.05 concentrations, material-a have (see Fig. 3a) an irregular leaf-like structure, material-b (see Fig. 3b), and material-c (see Fig. 3c) has an irregular shape. Surface morphology study of thin-film is an important tool to find out microstructures of thin films. Shape and size at nano/ micro scale modify the properties of matter and can have diverse applications. SEM micrographs show that the thin films were found to be continuous and crack-free. The average surface particle size was found to lie in a few micrometers range. By changing the speed of rotations morphology can also be modified. SEM micrographs reveal that it has different structures of different materials which may be due to different ligands tailored to get modified materials.

Thin-film prepared with wt.% 0.08 is shown in Figure 4. It is clear from Figure 4 that these micrographs have a continuous structure. All the micrographs show the formation of well-defined uniform films. In our work, we observed that SEM micrographs have surface defects resulting in polycrystals because it depicts interfaces grain-boundary-grain and found that the spin coating method is suitable for making thin films on glass substrates for these new tailored organic semiconducting materials. These thin films are suitable for various applications like PV solar cells.

Material-a was prepared at two concentrations. Both the solutes were fully dissolved in chloroform. As the weight percentage increased from 0.05 to 0.08, the leaf liked structure's morphology changes to more denser structure with close packing. The free space shown in the wt.% is 0.05 film was disappeared as the wt % is 0.08. This may be due to the changed behavior which can be the result of increased weight percentage. Similar results are obtained for the second compound when concentration is altered as observed from the above figures. SEM observations were also correlated with XRD data. We found that both SEM micrographs and XRD graph shows that the material was in polycrystalline form. Successful fabrication of these flat layers of such newly tailored organic semiconductors by low-cost spin coating technique opens the possibility of upscaling these new materials for industrial applications.

3.3 Optical characterization by UV-Vis spectroscopy

UV-Visible absorption spectroscopy is a powerful characterization method for studying the optical properties of semiconductors. The optical properties of thin films are very important to decide the applicability of materials in optoelectronic applications. To investigate the optical properties of these new tailored organic semiconductor thin films prepared at different concentrations, and the absorbance was measured in the wavelength range 200 nm to 1100 nm. The value of the bandgap is calculated from the absorption edge of thin films [55]. Band-gap is one of the most important parameters of semiconductors to decide further the applications. For the development of the electronic band structures of thin films of a material, it is necessary to determine the energy gap. The most common

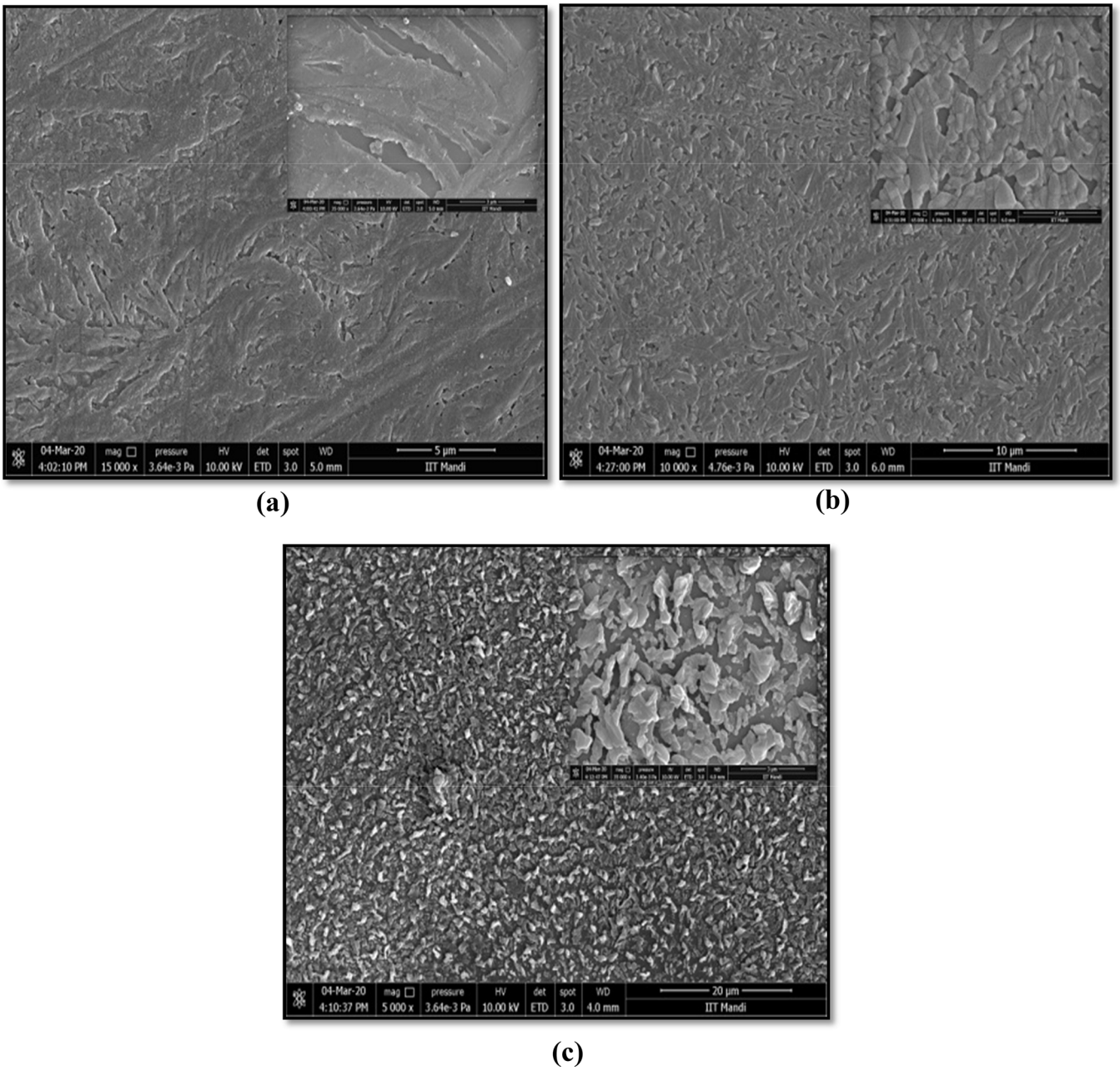

Fig. 3. SEM images of **(a)** material-a: (Anthracen-9-yl)methylene naphthalene-1-amine with wt% 0.05, **(b)** material-b: 4-(anthracen-9-ylmethylene amino)-1,5-dimethyl-2-phenyl-1H-pyrazol-3-one wt% 0.05, and **(c)** material-c: N-(anthracen-9-ylmethyl)-3,4-dimethoxyaniline with wt% 0.05.

method was to find out the bandgap of semiconductors by measuring the optical absorption and transmission [56,57]. The absorption graphs were drawn and the corresponding peaks were observed. We find that the absorption peaks lie in the UV and visible regions for these new tailored organic structures (Fig. 5).

Moreover, Tauc relation [58] is used to estimate the value of the bandgap of these thin films from the absorption spectra.

$$\alpha hv = A'\left(hv - E_g\right)^n.$$

In Tauc relation, $\alpha = 2.303\mathrm{A/t}$, and is known as the absorption coefficient, A is denoted for absorbance, t is indicated as a path length of the wave and that is equal to the thickness of the film, A' is represented as the proportionality constant, Eg is the bandgap, hv is the photon energy, and the value of $n = 1/2$ for direct bandgap and 2 ($n = 2$) for indirect bandgap semiconductors. Against the photon energy (hv), the best linear relationship was obtained by plotting $(\alpha hv)^2$. The line fit to the $(\alpha hv)^2$ versus hv plot is obtained by fitting a straight line to the linear portion of the curve. The value of the optical band gap was

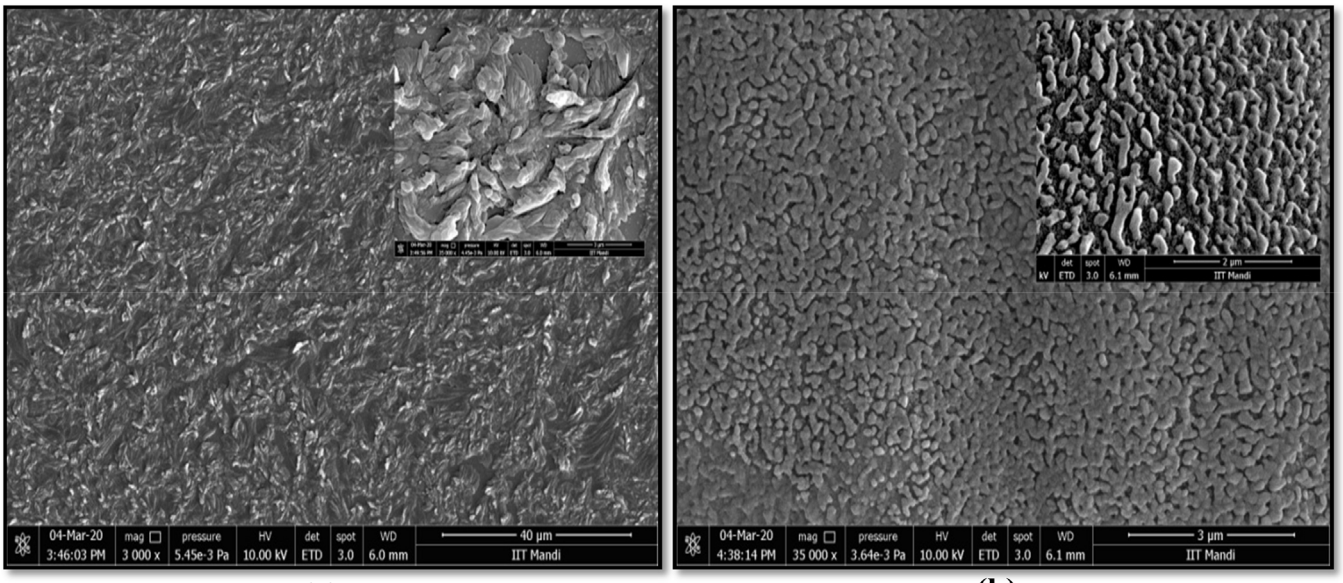

Fig. 4. SEM images of **(a)** material-a: (Anthracen-9-yl)methylene naphthalene-1-amine with wt% 0.08, and **(b)** material-b: 4-(anthracen-9-ylmethylene amino)-1,5-dimethyl-2-phenyl-1H-pyrazol-3-one with wt% 0.08.

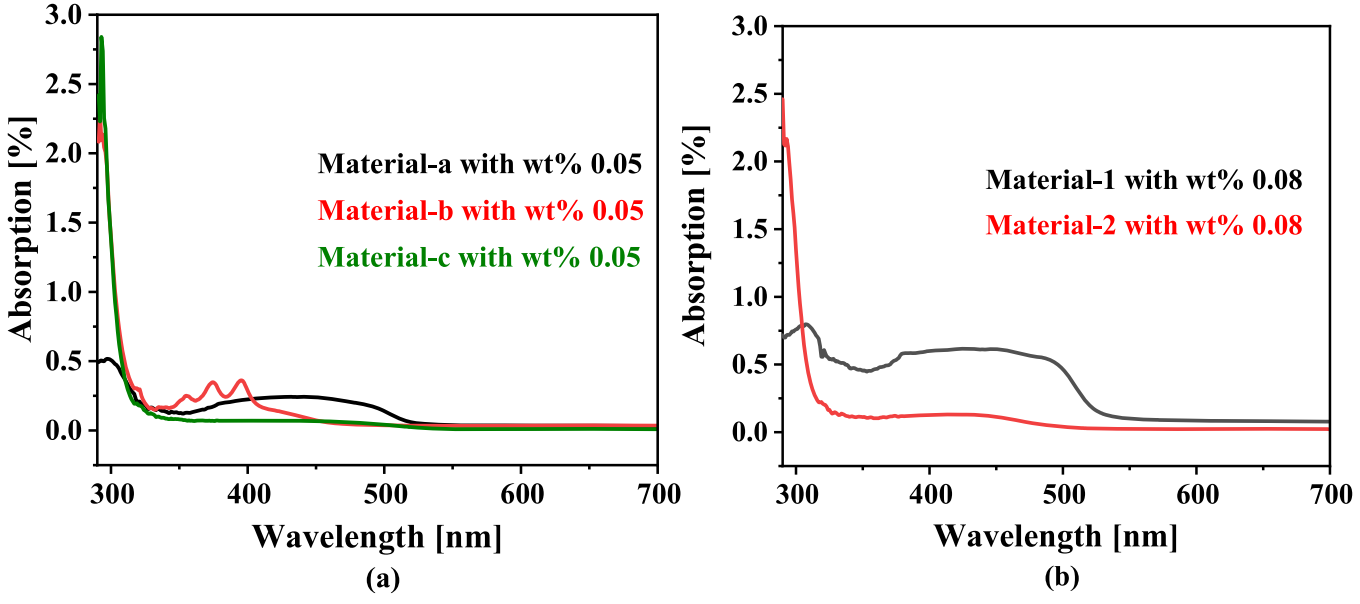

Fig. 5. Absorption spectra of **(a)** material-a: (Anthracen-9-yl)methylene naphthalene-1-amine with wt% 0.05, material-b: 4-(anthracen-9-ylmethylene amino)-1,5-dimethyl-2-phenyl-1H-pyrazol-3-one wt% 0.05, material-c: N-(anthracen-9-ylmethyl)-3, 4-dimethoxyaniline with wt% 0.05, **(b)** material-a: (Anthracen-9-yl)methylene naphthalene-1-amine with wt% 0.08, material-b: 4-(anthracen-9-ylmethylene amino)-1,5-dimethyl-2-phenyl-1H-pyrazol-3-one wt% 0.08.

investigated from the value of the intercept of the straight line at $\alpha = 0$. Graphs were drawn for each sample are shown below.

In our work as observed from Figure 6, the highest bandgap for organic semiconductor thin film was found to be 2.65 eV for material-c. For organic thin films of material-a, material-b having wt.% 0.05 the band gap was found to be 2.52 eV and 2.36 eV respectively. For organic thin films having wt.% 0.08, the bandgap was found to be 2.35 eV and 2.18 eV. We observed that the bandgap decreases by increasing the wt.% from 0.05 to 0.08. The small variation of bandgap shows that bandgap energy might originate from the defects in organic thin films. These investigations reveal that the different structures of different organic material and using different concentrations was the main reason of the variation of the bandgap of

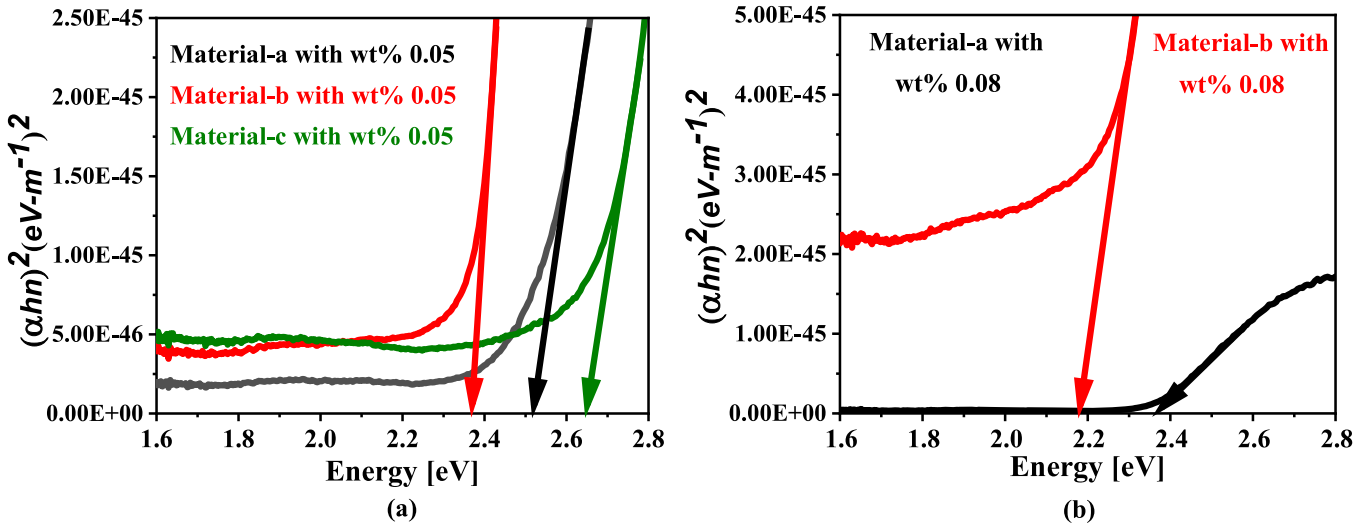

Fig. 6. Band graph of (a) material-a: (Anthracen-9 yl)methylene naphthalene-1-amine with wt% 0.05, material-b: 4-(anthracen-9-ylmethylene amino)-1,5-dimethyl-2-phenyl-1H-pyrazol-3-one with wt% 0.05, material-c: N-(anthracen-9-ylmethyl)-3,4-dimethoxyaniline with wt% 0.05 of solute and (b) material-a: (Anthracen-9-yl)methylene naphthalene-1-amine with wt% 0.08, material-b: 4-(anthracen-9-ylmethylene amino)-1,5-dimethyl-2-phenyl-1H-pyrazol-3-one with wt% 0.08 solute.

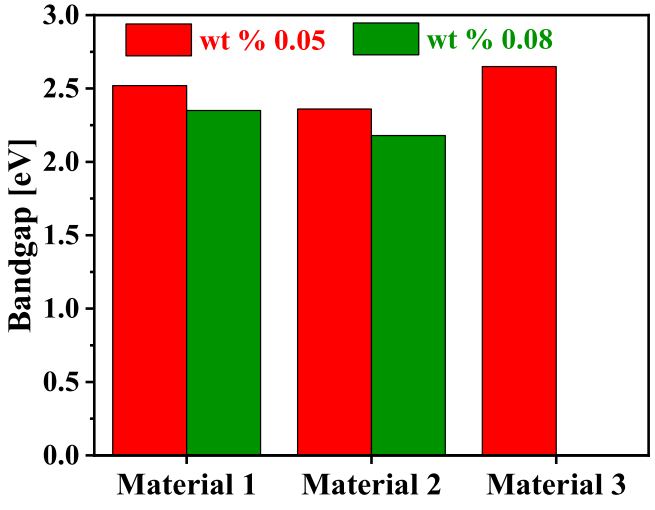

Fig. 7. Systematic representations of variation of band gaps.

synthesized samples and hence modified the optical properties. Yuan et al. [59] previously suggested that band gap can also be engineered under high pressure. But in our studies, we found that parameters like change in concentration can also engineer the band of organic materials. These tuned band gaps are possibly suitable for capturing more light energy as compared to other traditional organic materials which have a bandgap around 3 eV because of solar spectrum distribution. Thus, these films are suitable for optoelectronic devices such as solar cells. The organic thin-film having a bandgap of 2.18 eV is possibly suitable for making OFET devices. Such tuning of bandgap toward IR from traditional UV region makes these new tailored materials suitable candidates of harnessing better solar spectrum including other optoelectronic applications like OLED, OFET, etc and also open the possibility of futher engineering.

Comparative studies have also been done on the basis of results (Fig. 7). The bandgap was shown to be decreased while increasing the weight percentage from 0.05 to 0.08 for (Anthracen-9-yl)methylenenaphthalene-1-amine and 4-(anthracen-9-ylmethyleneamino)-1,5-dimethyl-2-phenyl-1H-pyrazol-3-one (2.35 eV and 2.18 eV). Besides, these three materials are organic compounds and which contain either nitrogen or oxygen and nitrogen along with hydrocarbons. Very recently, it is theoretically and experimentally proved that oxygen and nitrogen linker-controlled chains strongly influence the polymer's electronic structure [60]. The presence of oxygen and nitrogen in our material looks the reason for the slight variation of the bandgap. Further studies in light of variation of concentration need to be done for bandgap engineering.

4 Conclusion

This work demonstrates the new tailored organic semiconductor materials thin-film of (Anthracen-9-yl) methylenenaphthalene-1-amine; 4-(anthracen-9-ylmethylene amino)-1,5-dimethyl-2-phenyl-1H-pyrazol-3-one; and N-(anthracen-9-ylmethyl)-3,4-dimethoxyaniline by spin coating method with changing concentration such as 0.05 wt.% and 0.08 wt.%. The structural, morphological, and optical properties of prepared organic semiconductor's thin films are studied by X-ray diffraction (XRD), Scanning electron microscopy (SEM) and UV-Visible spectroscopy technique. The XRD graphs suggest that the organic thin films have broad peaks depicting their nanocrystalline nature. Along with this, the particle size of three different materials with wt.% 0.05 and 0.08 has increased which concludes that the changing concentration of material and its structure is beneficial for obtaining the nanomaterials that are probably suited for the solar cells. The SEM images suggest evidence of interconnected

uniform particles on the glass substrate. In addition, SEM images of annealed organic thin films on glass substrate at wt.% 0.05 concentrations show the irregular leaf-like structure and irregular shape. On the other hand, thin-film prepared with wt.% 0.08 is shown micrographs have a continuous structure which means the formation of well-defined uniform films. Overall, we observed that both SEM and XRD data show that the material was in polycrystalline form. Moreover, the bandgap of these new materials is engineered to about 2.2 eV which confirms the suitability of these new tailored lightweight materials for harnessing solar spectrum as compared to other traditional inorganic and organic structures. While changing the weight percentage, it is observed that the bandgap is decreasing. And finally, we can say that a low-cost spin coating method appears to be suitable for processing these new tailored organic semiconductors and can have the potential for industrial applications in future technology based on organics.

Author contribution statement

Dinesh Pathak planned the whole idea, experiments, manuscript and mentored this research work. Sanjay and Vaneet Kumar written the manuscript with analysis. Sonali and Jibin Thomas performed experiment and collected data with Praveen Kumar. Navneet Kaur synthesized the new organic structures which are explored here for optoelectronics applications.

References

1. F. Yang, S. Cheng, X. Zhang, X. Ren, R. Li, H. Dong, W. Hu, Adv. Mater. **30**, 1702415 (2018)
2. H. Lee, J.H. Kim, K.P. Dhakal, J.W. Lee, J.S. Jung, J. Joo, J. Kim, Appl. Phys. Lett. **101**, 113103 (2012)
3. G.P. Neupane, K.P. Dhakal, E.H. Cho, B.-G. Kim, S. Lim, J. Lee, C. Seo, Y.B. Kim, M.S. Kim, J. Kim, J. Joo, J. Kim, Electron. Mater. Lett. **11**, 741 (2015)
4. M.M. Ling, Z. Bao, Chem. Mater. **16**, 4824 (2004)
5. C. Reese, M. Roberts, M.M. Ling, Z. Bao, Mater. Today **7**, 20 (2004)
6. G. Horowitz, Adv. Mater. **10**, 365 (1998)
7. C.D. Sheraw, J.A. Nichols, D.J. Gundlach, J.R. Huang, C.C. Kuo, H. Klauk, T.N. Jackson, M.G. Kane, J. Campi, F.P. Cuomo, B.K. Greening, in Proc. IEEE Int. Electron Devices Meet. 619 (2000)
8. T.N. Jackson, IEEE Int. Semicond. DeVice Res. Symp. 340 (2001)
9. C.D. Dimitrakopoulos, P.R.L. Malenfant, Adv. Mater. **14**, 99 (2002)
10. T. Adhikari, S.R. Bobbara, J.M. Nunzi, O. Lebel, Org. Electron. **53**, 74 (2018)
11. T. Adhikari, Z.G. Rahami, J.M. Nunzi, O. Lebel, Org. Electron. **34**, 146 (2016)
12. J. Liu, S. Chen, D. Qian, B. Gautam, G. Yang, J. Zhao, J. Bergqvist, F. Zhang, W. Ma, H. Ade, O. Inganäs, K. Gundogdu, F. Gao, H. Yan, Nat. Energy **1**, 16089 (2016)
13. T. Adhikari, J.M. Nunzi, O. Lebel, Org. Electron. **49**, 382 (2017)
14. C.W. Tang, S.A. VanSlyke, C.H. Chen, J. Appl. Phys. **65**, 3610 (1989)
15. T. Tsutsui, S. Saito, Intrinsically Conducting Polymers: An Emerging Technology NATO ASI Ser., Ser. E **246**, 123 (1993)
16. Z. Bao, A.J. Lovinger, J. Brown, J. Am. Chem. Soc. **120**, 207 (1998)
17. P.R.L. Malenfant, C.D. Dimitrakopoulos, J.D. Gelorme, L.L. Kosbar, T.O. Graham, Appl. Phys. Lett. **80**, 2517 (2002)
18. Y. Lin, D.J. Gundlach, S.F. Nelson, T.N. Jackson, IEEE Electr. Device Lett. **18**, 606 (1997)
19. D.J. Gundlach, Y.Y. Lin, T.N. Jackson, S.F. Nelson, D.G. Schlom, IEEE Electr. Device Lett. **18**, 87 (1997)
20. Y. Qiu, Y. Hu, G. Dong, L. Wang, J. Xie, Y. Ma, Appl. Phys. Lett. **83**, 1644 (2003)
21. H. Meng, F. Sun, M.B. Goldfinger, G.D. Jaycox, Z. Li, W.J. Marshall, G.S. Blackman, J. Am. Chem. Soc. **127**, 2406 (2005)
22. Y.Y. Lin, D.I. Gundlach, S.F. Nelson, T.N. Jackson, IEEE Trans. Electr. Dev. **44**, 1325 (1997)
23. H. Uoyama, K. Goushi, K. Shizu, H. Nomura, C. Adachi, Nature **492**, 234 (2012)
24. T.N. Jackson, Y.Y. Lin, D.J. Gundlach, H. Klauk, IEEE J. Selected Top. Quant. Electr. **4**, 100 (1998)
25. S. Reineke, F. Lindner, G. Schwartz, N. Seidler, K. Walzer, B. Lüssem, K. Leo, Nature **459**, 234 (2009)
26. T. Adhikari, J.M. Nunzi, O. Lebel, Org. Electron. **48**, 230 (2017)
27. T. Adhikari, P. Solanke, D. Pathak, T. Wagner, F. Bureš, T. Reed, J.M. Nunzi, Opt. Mater. **69**, 312 (2017)
28. L.S. Liao, K.P. Klubek, C.W. Tang, Appl. Phys. Lett. **84**, 4 (2004)
29. M. Gross, D.C. Muller, H.G. Nothofer, U. Scherf, D. Neher, C. Brauchle, K. Meerholz, Nature **405**, 661 (2000)
30. K.H. Yim, G.L. Whiting, C.E. Murphy, J.J.M. Halls, J.H. Burroughes, R.H. Friend, J.S. Kim, Adv. Mater. **20**, 3319 (2008)
31. A.J. Heeger, S. Kivelson, J.R. Schrieffer, W.P. Su, Rev. Mod. Phys. **60**, 781 (1988)
32. Y.W. Park, A.J. Heeger, J. Chem. Phys. **73**, 946 (1980)
33. M.T. Bernius, M. Inbasekaran, J. O'Brien, W. Wu, Adv. Mater. **12**, 1737 (2000)
34. G.L. Schulz, X. Chen, S. Holdcroft, Appl. Phys. Lett. **94**, 023302 (2009)
35. I.I. Fishchuk, A. Kadaschuk, S.T. Hoffman, S. Athanasopoulos, J. Genoe, H. Bassler, A. Kohler, Phys. Rev. B **88**, 125202 (2013)
36. N. Kaur, M. Singh, D. Pathak, T. Wagner, J.M. Nunzi, Synth. Met. **190**, 20 (2014)
37. D. Pathak, T. Wagner, T. Adhikari, J.M. Nunzi, Synth. Met. **199**, 87 (2015)
38. U. Jabeen, T. Adhikari, S.M. Shah, D. Pathak, T. Wagner, J.M. Nunzi, Eur. Phys. J. Appl. Phys. **78**, 34809 (2017)
39. B. Fan, D. Zhang, M. Li, W. Zhong, Z. Zeng, L. Ying, F. Huang, Y. Cao, Science China Chem. **62**, 746 (2019)
40. G. Gu, Z. Zhang, H. Dang, Mater. Res. Bull. **39**, 1037 (2004)
41. S. Kumar, S. Saralch, D. Pathak, Eur. Phys. J. Appl. Phys. **84**, 20301 (2018)
42. B. Wang, T. Zhu, L. Huang, T.L.D. Tam, Z. Cui, J. Ding, L. Chi, Org. Electron. **24**, 170 (2015)

43. G. Gu, P.E. Burrows, S. Vankatesh, S.R. Forrest, M.E. Thompson, Opt. Lett. **22**, 173 (1997)
44. V.E. Chong, Y. Park, Y. Gao, M.G. Mason, C.W. Tang, J. Vac. Sci. Technol. A **16**, 1838 (1998)
45. D.J. Gundlach, J.A. Nichols, L. Zhou, T.N. Jackson, Appl. Phys. Lett. **80**, 2925 (2002)
46. H. Biederman, J. Vac. Sci. Technol. A **18**, 1642 (2002)
47. S.Y. Park, H.R. Kim, Y.J. Kang, D.H. Kim, J.W. Kang, Sol. Energy Mater. Sol. Cells **94**, 2332 (2010)
48. A.U. Ubale, Mater. Chem. Phys. **121**, 555 (2010)
49. S. Kumar, S. Saralch, U. Jabeen, D. Pathak, Metal oxides for energy applications, in *Colloidal Metal Oxide Nanoparticles* (Elsevier, Amsterdam) (2020) pp. 471–504
50. Y. Diao, L. Shaw, Z. Bao, S.C.B. Mannsfeld, Energy Environ. Sci. **7**, 2145 (2014)
51. L.L. Chua, P.K.H. Ho, H. Sirringhaus, R.H. Friend, Adv. Mater. **16**, 1609 (2004)
52. B.K. Kundu, P. Mandal, B.G. Mukhopadhyay, R. Tiwari, D. Nayak, R. Ganguly, S. Mukhopadhyay, Sens. Actuators B **282**, 347 (2019)
53. S. Janaa, S. Dalapati, M.A. Alamb, N. Guchhait, Spectrochim. Acta Part A **92**, 131 (2012)
54. V. Drits, J. Środoń, D.D. Eberl, Clays Clay Miner. **45**, 461 (1997)
55. M.S. Shinde, P.B. Ahirrao, I.J. Patil, R.S. Patil, Indian J. Pure Appl. Phys. **50**, 657 (2012)
56. Z.R. Khan, M.S. Khan, M. Zulfequar, M.S. Khan, Mater. Sci. Applicat. **2**, 340 (2011)
57. C.X. Xu, X.W. Sun, J. Cryst. Growth **277**, 330 (2005)
58. J. Tauc, Optical Properties of Solids, Abeles, North-Holland, Amsterdam (1972)
59. Y. Yuan, X.F. Liu, X. Ma, X. Wang, X. Li, J. Xiao, X. Li, H.L. Zhang, L. Wang, Adv. Sci. **6**, 1900240 (2019)
60. Y. Wang, M.K. Bayazit, S.J.A. Moniz, Q. Ruan, C.C. Lau, N. Martsinovich, J. Tang, Energy Environ. Sci. **10**, 1643 (2017)

Cite this article as: Dinesh Pathak, Sanjay Kumar, Sonali Andotra, Jibin Thomas, Navneet Kaur, Praveen Kumar, Vaneet Kumar, New tailored organic semiconductors thin films for optoelectronic applications, Eur. Phys. J. Appl. Phys. **95**, 10201 (2021)